



# Influence of septic system wastewater treatment on titanium dioxide nanoparticle subsurface transport mechanisms

Travis Waller<sup>1</sup> · Ian M. Marcus<sup>1</sup> · Sharon L. Walker<sup>2</sup>

Received: 7 March 2018 / Revised: 1 May 2018 / Accepted: 9 May 2018 / Published online: 4 June 2018  
© Springer-Verlag GmbH Germany, part of Springer Nature 2018

## Abstract

Engineered nanomaterials (ENMs) are commonly incorporated into food and consumer applications to enhance a specific product aspect (i.e., optical properties). Life cycle analyses revealed ENMs can be released from products during usage and reach wastewater treatment plants (WWTPs), with titanium dioxide (TiO<sub>2</sub>) accounting for a large fraction. As such, food grade (FG) TiO<sub>2</sub>, a more common form of TiO<sub>2</sub> in wastewater, was used in this study. Nanomaterials in WWTPs have been well characterized, although the problematic septic system has been neglected. Elution and bioaccumulation of TiO<sub>2</sub> ENMs from WWTPs in downriver sediments and microorganisms has been observed; however, little is known about mechanisms governing the elution of FG TiO<sub>2</sub> from the septic drainage system. This study characterized the transport behavior and mechanisms of FG TiO<sub>2</sub> particles in porous media conditions after septic waste treatment. FG and industrial grade (IG) TiO<sub>2</sub> (more commonly studied) were introduced to septic tank effluent and low-ionic strength electrolyte solutions prior to column transport experiments. Results indicate that FG TiO<sub>2</sub> aggregate size (200–400 nm) remained consistent across solutions. Additionally, elution of FG and IG TiO<sub>2</sub> was greatest in septic effluent at the higher nanoparticle concentration (100 ppm). FG TiO<sub>2</sub> was well retained at the low (2 ppm) concentration in septic effluent, suggesting that particles that escape the septic system may still be retained in drainage field before reaching the groundwater system, although eluted particles are highly stabilized. Findings provide valuable insight into the significance of the solution environment at mediating differences observed between uniquely engineered nanomaterials.

**Keywords** Food grade · Titanium dioxide · Wastewater · Groundwater · Filtration

## Introduction

Engineered nanomaterials (ENMs) represent an expanding class of nanosized materials that are used in numerous applications for matrix stabilization and enhancement of optical properties [1], including consumer products such as foods

[2–4] and cosmetics, coatings, pharmaceuticals, pigments, paints, and personal care products [4, 5]. Interestingly, multiple studies of the life cycle of consumer product-based ENMs have reported that nanomaterials can be released from products during the lifespan of their usage with many reaching full-scale wastewater treatment plants (WWTPs) [5, 6]. Titanium dioxide (TiO<sub>2</sub>) ENMs, for example, are estimated to account for a large fraction [40–50%] [5] of engineered nanomaterials reaching WWTPs, due to frequent usage and release from foods and consumer products [2, 3, 5, 7–9].

Full-scale WWTPs reduce the loading of organics, nutrients, and other potential environmental contaminants before wastewater is released into the environment [10]. Two to four primary treatment stages are typically incorporated at centralized facilities: preliminary treatment to remove large objects damaging to the plant, primary treatment using physical removal processes (i.e., sedimentation), secondary treatment using biological or chemical processes for nutrient removal, and tertiary treatment to further remove organics, pathogens,

---

Published in the topical collection *Analytical Developments in Advancing Safety in Nanotechnology* with guest editors Lisa Holland and Wenwan Zhong.

✉ Sharon L. Walker  
swalker@engr.ucr.edu

<sup>1</sup> Department of Chemical and Environmental Engineering, University of California, Riverside, A220 Bourns Hall, Riverside, CA 92521, USA

<sup>2</sup> Department of Chemical and Environmental Engineering, University of California, Riverside, A237 Bourns Hall, Riverside, CA 92521, USA

and parasites [11]. Nanomaterials tend to aggregate and associate with biosolids within full-scale WWTPs prior to sedimentation from treated effluent [12, 13]. However, in certain cases, though colloidal-sized TiO<sub>2</sub> particles are well removed, up to 70% of nano-TiO<sub>2</sub> was eluted from the full-scale WWTP [14]. Additionally, TiO<sub>2</sub> nanoparticles released from WWTPs can remain bioavailable, which is evidenced by accumulation of small quantities (< 5 µg/L) in fish just downriver of the treatment facility [15]. Notably, TiO<sub>2</sub> ENMs detected in receiving waters were determined to be engineered and non-naturally occurring [15]. These studies indicate that nanosized, engineered TiO<sub>2</sub> can remain an environmental concern after leaving full-scale WWTPs.

Septic wastewater treatment systems, alternatively, are a simpler microbially driven, anaerobic digester utilizing only the sedimentation and filtration aspects of larger treatment operations [16]. Sedimentation of suspended solids and microbial degradation of organics occurs in the septic tank, and effluent slow trickle filtration occurs in the drainage field. Although septic systems are EPA regulated and effective when installed and maintained properly, they are often less rigorous than full-scale WWTPs [11] and shortcomings in design and maintenance lead to system failure [17]. Notably, TiO<sub>2</sub> and other ENMs well studied and characterized in full-scale WWTPs have largely been neglected in the onsite, septic systems [18]. TiO<sub>2</sub> ENMs in poorly maintained septic systems, as opposed to WWTPs, suggest the possibility of greater elution from the onsite system [19] and shifts the focus to nanoparticle behavior in the drainage field after septic treatment.

Nanoparticle fate and transport in porous media is dependent on both solution chemistry and inherent particle characteristics [20, 21]. TiO<sub>2</sub> nanoparticles characterized under idealized conditions indicated that food grade (FG) TiO<sub>2</sub>, which is more commonly used in foods and consumer products [4], possessed a different isoelectric point (IEP) than a more commonly studied form of TiO<sub>2</sub> (FG: pH 3.5; industrial grade: pH 6) [22]. Wastewater systems typically remain between pH 6 and 7, indicating that while industrial grade TiO<sub>2</sub> particles should be destabilized, FG TiO<sub>2</sub> should be stable with a negative charge based on IEP. Further, FG TiO<sub>2</sub> nanoparticles exhibit interesting stability across multiple ideal and complex solution conditions [23], potentially increasing its chances of remaining suspended in effluent eluted from the drainage field into the groundwater system. Essentially, transport mechanisms governing FG TiO<sub>2</sub> nanoparticle behavior in porous media after septic treatment are largely unknown and represent an important consideration regarding the environmental fate and transport of FG TiO<sub>2</sub>.

This study aimed to characterize the transport behavior and mechanisms of FG TiO<sub>2</sub> particles in porous media indicative of conditions in post septic waste treatment. Two forms of TiO<sub>2</sub> nanoparticles were utilized to assess the correlation between FG and a more commonly studied form of industrial

grade (IG) TiO<sub>2</sub>. Characterization of nanoparticles included particle size and mobility within each solution condition. Nanoparticle transport experiments were conducted using a cylindrical glass column wet packed with quartz sand grains. Breakthrough curves were then created to elucidate the influence of solution chemistry and particle concentration in FG TiO<sub>2</sub> porous media transport.

## Experimental protocols

### Nanoparticle selection and characterization

FG and IG TiO<sub>2</sub> were used, independently, for all experimental conditions of this study. Nanomaterial selection was largely determined by FG being a commonly found particle in domestic sewage [4, 5], while the IG was used in this study as a control, as a most commonly studied TiO<sub>2</sub> particle [22]. Interestingly, both grades have pathways to reach wastewater treatment facilities [4]. Food grade TiO<sub>2</sub> are commercially available particles provided via Arizona State University and have a primary particle size of 122 ± 48 nm and mostly anatase crystal structure (> 95%); additionally, the particle carries an inorganic phosphate coating [22]. Industrial grade TiO<sub>2</sub> are nanoparticles sourced from Sigma-Aldrich (Aeroxide TiO<sub>2</sub> P25; Evonik Degussa Corporation, Essen, DE) and possess a primary particle size of 21 nm and a compound crystal structure of 75% anatase and 25% rutile [22, 23]. The isoelectric point of FG TiO<sub>2</sub> is within the range of pH 3.5 to 4, while IG TiO<sub>2</sub> is pH 6 in 10 mM monovalent electrolyte solutions [22, 23].

Nanoparticles were prepared following previously described methods [24]. Briefly, a 200 ppm stock solution of TiO<sub>2</sub> nanoparticles was prepared and sonicated for 30 min prior to beginning experiments, then another 30 s just before each characterization experiment. Nanoparticle concentrations of 2 and 100 ppm were selected to approximate environmentally relevant levels and nanoparticle concentrations used in prior studies [21]. Although 0.2 ppm represents the high level of TiO<sub>2</sub> in this environment [15, 25], 2 ppm was selected due to optical resolution limitations of the spectrophotometer.

Nanoparticle characterization included both hydrodynamic diameter and zeta-potential (ZP) measurements across each solution condition and TiO<sub>2</sub> concentration. Hydrodynamic diameter was determined using dynamic light scattering (ZetaPALS, Holtzville, NY, USA) at a wavelength of 661 nm and a scattering angle of 90°. ZP was calculated using the Smoluchowski equation [20] converted using electrophoretic mobility measurements (ZetaPALS, Holtzville, NY, USA).

### Solution chemistry and characterization

Treated wastewater released from septic treatment systems must first trickle through a drainage field of porous medium

before entering the groundwater system [16]. Therefore, septic system wastewater effluent was the primary solution utilized in this study to replicate conditions present within the drainage field. Septic effluent was produced using a bench-scale model septic tank and human colon that provided human fecal matter [18, 23, 26]. The water quality of the septic effluent was evaluated via conductivity ( $570 \mu\text{S}/\text{cm}$ ), pH (7.6), microbial concentration ( $5.01 \times 10^8 \pm 6 \times 10^7$  cells/mL), turbidity ( $9.9 \pm 0.8$  NTU), and chemical oxygen demand ( $315.9 \pm 12.4$  mg/L). Additionally, 4 mM KCl with pH adjusted to 7.6 and 10 mM KCl (no adjustment, pH 6) were two, separately tested, monovalent electrolyte suspensions used to indicate the significance of organic matter and increased ionic strength, respectively. Conductivity is the measure of charge transferring capacity of a solution and an estimate of IS. Calibration curves were created to determine the molar concentration of KCl equaling septic effluent conductivity with the result being 4 mM. The transport properties of six nanoparticle suspensions were tested independently in triplicate using sand columns. The six suspensions comprised two grades (food and industrial) of  $\text{TiO}_2$  nanoparticles independently suspended in three solutions (septic effluent, 4 mM KCl (pH 7.6), and 10 mM KCl (pH 6)). Solution chemistries provided a comparison of the role played by organic material remaining in the septic system (4 mM KCl, pH 7.6) and for the consideration of FG  $\text{TiO}_2$  filtration behavior in relation to commonly studied literature conditions (10 mM KCl).

### Column transport experiments

Column transport experiments were conducted to elucidate the porous media behavior of FG  $\text{TiO}_2$ . A borosilicate glass cylinder of dimensions 1.5 cm inner diameter and 5 cm length was wet packed with  $275 \mu\text{m}$  ultrapure quartz sand, resulting in 0.46 porosity to simulate filtration through a septic drain field [16]. Column operation and setup are presented in greater detail elsewhere [21]. Flow rate was maintained at 2 mL/min which is commonly found in trickle flows and slow sand grain filtration [10]. Greater than 10 pore volumes (PV) of Millipore deionized water ( $18.2 \text{ M}\Omega$  at  $25^\circ\text{C}$ ) were flushed through the column after sand was wet packed. This initial flush was followed by greater than 10 PV of the electrolyte solution (4 mM KCl, 10 mM KCl, or septic effluent; without nanoparticles) to fully saturate the porous media in the respective background solution. Six PV of  $\text{TiO}_2$  nanoparticle suspensions (background electrolyte solutions spiked with  $\text{TiO}_2$ ) was then introduced followed by another 6 PV of the nanoparticle-free background electrolyte solution. Septic effluent was obtained from the column using 15-mL centrifuge tubes and fraction collector (CF 1 Fraction Collector, Spectrum Chromatography, Houston, TX, USA). The nanoparticle suspensions were constantly sonicated and stirred during  $\text{TiO}_2$  introduction.

### DLVO calculations

Derwin-Landau-Verwey-Overbeek (DLVO) theory was applied to provide insight on deposition mechanisms of both FG and IG  $\text{TiO}_2$  in this porous media system. DLVO theory allowed for the determination of the significance of electrostatic repulsion and van der Waals interactions on the  $\text{TiO}_2$  nanoparticles and quartz sand collector comprising the transport column. Sphere plate geometry was assumed for this  $\text{TiO}_2$  quartz system due to the comparatively smaller diameters of nanoparticles compared with a quartz sand collector grain size of  $\sim 250\text{--}300 \mu\text{m}$ . DLVO theory was applied using the following equations for electrostatic repulsion ( $V_{\text{edl}}$ ) (Eq. 1) and van der Waals forces ( $V_{\text{VDW}}$ ) (Eq. 2):

$$V_{\text{edl}} = \pi\epsilon_0\epsilon_{\text{ap}} \left\{ 2\psi_p\psi_c \ln \left[ \frac{1 + \exp(-kh)}{1 - \exp(-kh)} \right] + (\psi_c^2 + \psi_p^2) \ln[1 - \exp(-2kh)] \right\} \quad (1)$$

$$V_{\text{VDW}} = \frac{A_{102}a_p}{6h} \left( 1 + \frac{14h}{\lambda} \right)^{-1} \quad (2)$$

where the following assumed parameters were utilized from previously published and measurements from this study: permittivity constant of free space ( $\epsilon_0$ ) was  $8.854 \times 10^{-12} \text{ C/V/m}$ , the dielectric constant of water ( $\epsilon$ ) was 78.5, and surface potentials ( $\psi$ ) determined by EPM measurements were transformed to zeta-potentials using the Smoluchowski equation for the particle ( $p$ ) and collector ( $c$ ) [27]. Inverse Debye length and separation distance are denoted by  $\kappa$  and  $h$ , respectively [20]. The Hamaker constant ( $A_{102}$ ) selected for a quartz  $\text{TiO}_2$  system was  $10^{-20}$  [28], and the particle radius ( $a_p$ ) was populated by hydrodynamic diameter values (Fig. 1). Lastly, characteristic wavelength ( $\lambda$ ) was assumed to be 100 nm [27].

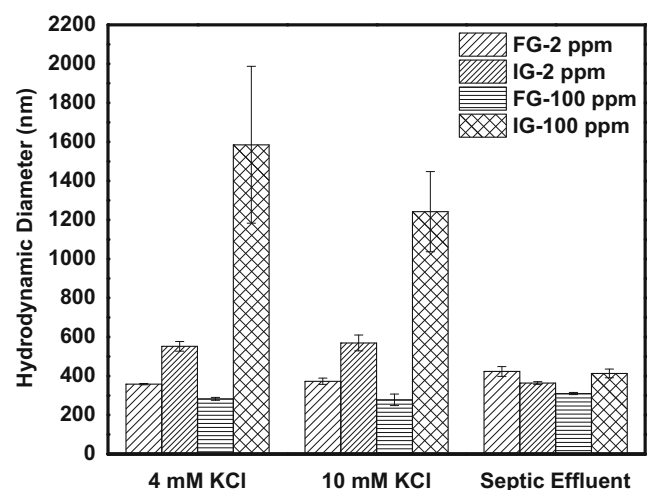


Fig. 1 Hydrodynamic diameters for food grade (FG) and industrial grade (IG) titanium dioxide particles in 4 mM KCl at pH 7.6, 10 mM KCl at pH 6, and septic effluent at pH 7.6. Errors bars represent standard deviation of triplicate measurements

## Statistical analysis

Student's *t* test was used to determine the statistical significance for nanoparticle characterization and breakthrough curves. An alpha value of 0.05 ( $p$  value  $< 0.05$ ) indicated statistically significant differences resulted in the FG or IG TiO<sub>2</sub> nanoparticle suspensions.

## Results

### Nanoparticle characterization

The hydrodynamic diameter of each type of TiO<sub>2</sub> particle is presented in Fig. 1. Notably, IG and FG TiO<sub>2</sub> vary little in their respective mean diameters between both KCl suspensions. Industrial grade TiO<sub>2</sub> developed a significantly larger ( $p < 0.05$ ) hydrodynamic diameter than FG TiO<sub>2</sub> in both 4 and 10 mM KCl, which is similar to previous research that found IG to form larger aggregates than FG [23]. Contrary size relationships by particle concentration were observed in KCl between FG and IG TiO<sub>2</sub> hydrodynamic diameters with 100 ppm IG TiO<sub>2</sub>, developing significantly larger aggregates than 2 ppm ( $> 1200$  to  $< 600$  nm, respectively), while 100 ppm FG TiO<sub>2</sub> formed significantly smaller aggregates than 2 ppm ( $< 282.5 \pm 7.5$  to  $> 358.3 \pm 3.2$  nm). Suspending the particles in septic effluent resulted in the development of very similar sizes between IG and FG TiO<sub>2</sub>. Septic effluent appears to stabilize IG TiO<sub>2</sub> particle sizes compared to both KCl solutions, while the size FG TiO<sub>2</sub> was determined to be independent of solution chemistry.

The electrophoretic mobility for both grades of TiO<sub>2</sub> particles suspended in the three solution chemistries is presented in Fig. 2. The EPM of FG TiO<sub>2</sub> was negative

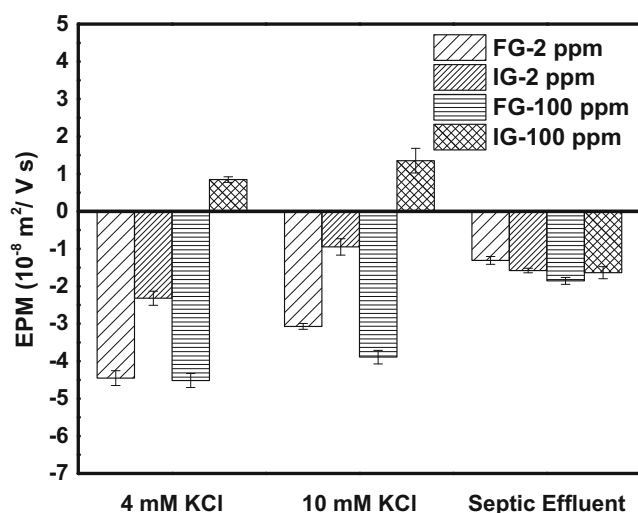


**Fig. 2** Electrophoretic mobility (EPM) for food grade (FG) and industrial grade (IG) titanium dioxide particles in 4 mM KCl at pH 7.6, 10 mM KCl at pH 6, and septic effluent at pH 7.6. Errors bars represent standard deviation of triplicate measurements

in all three solution conditions, and the value was independent of particle concentration. The greatest magnitude of EPM for FG was the 4 mM KCl solution, followed by the 10 mM suspension, while the FG suspended in the septic effluent had the lowest EPM. The IG particle EPM trends were similar across the two KCl suspensions. The low-concentration IG particles had negative EPM values, while those with higher concentrations had positive EPM values, yet irrespective of concentration, the IG particles developed equal, negative, and lower-magnitude EPM values when suspended in septic effluent (Fig. 2). Indeed, both grades of TiO<sub>2</sub> at both concentrations exhibited no differences in EPM when suspended in septic effluent. Septic effluent may exhibit a capacity for EDL compression even at low IS (570  $\mu$ S/cm,  $\sim 4$  mM) as both TiO<sub>2</sub> types and concentrations exhibit reduced EPM from either KCl solution [29].

### Column transport experiments

Breakthrough curves for food and industrial grade TiO<sub>2</sub> in each solution condition are provided in Fig. 3. Results indicate that FG TiO<sub>2</sub> was eluted more than IG in 4 mM KCl although in 10 mM KCl, both nanoparticle types were well retained (Fig. 3a, b). Nanoparticle concentration had little effect on IG retention in 10 mM KCl except in the case of 100 ppm IG TiO<sub>2</sub> where a small increase in particles eluted was observed ( $0.1 \pm 0.0$ ). Conversely, FG TiO<sub>2</sub> was far more impacted by particle concentration where FG 100 ppm (max  $0.4 \pm 0.0$ ) was much greater than FG 2 ppm (max  $0.0 \pm 0.0$ ) when suspended in 4 mM KCl. In septic effluent, differences in nanoparticle behavior were observed for both FG and IG TiO<sub>2</sub> when compared to the monovalent solutions (Fig. 3c). Septic effluent resulted in high elution values for all nanoparticles and concentrations except for FG 2 ppm. Notably, IG TiO<sub>2</sub> displayed an increased tendency for elution than those observed in 4 and 10 mM KCl. TiO<sub>2</sub> particle concentration played a major role under septic effluent conditions as both IG and FG TiO<sub>2</sub> exhibited similar behavior at the 100 ppm TiO<sub>2</sub> concentrations, and poor retention was observed at 100 ppm (max  $0.8 \pm 0.1$ ) compared to 2 ppm (max  $0.1 \pm 0.0$ ). Results indicate that septic effluent conditions facilitate increased elution of FG and IG TiO<sub>2</sub> nanoparticles compared to the monovalent electrolyte suspensions, though high retention is observed at environmentally relevant concentrations ( $< 2$  ppm).

### DLVO calculations

Total interaction energy profiles for food and industrial grade TiO<sub>2</sub> developed for 4 and 10 mM KCl are presented in Fig. 4 as a function of nanoparticle concentration and separation

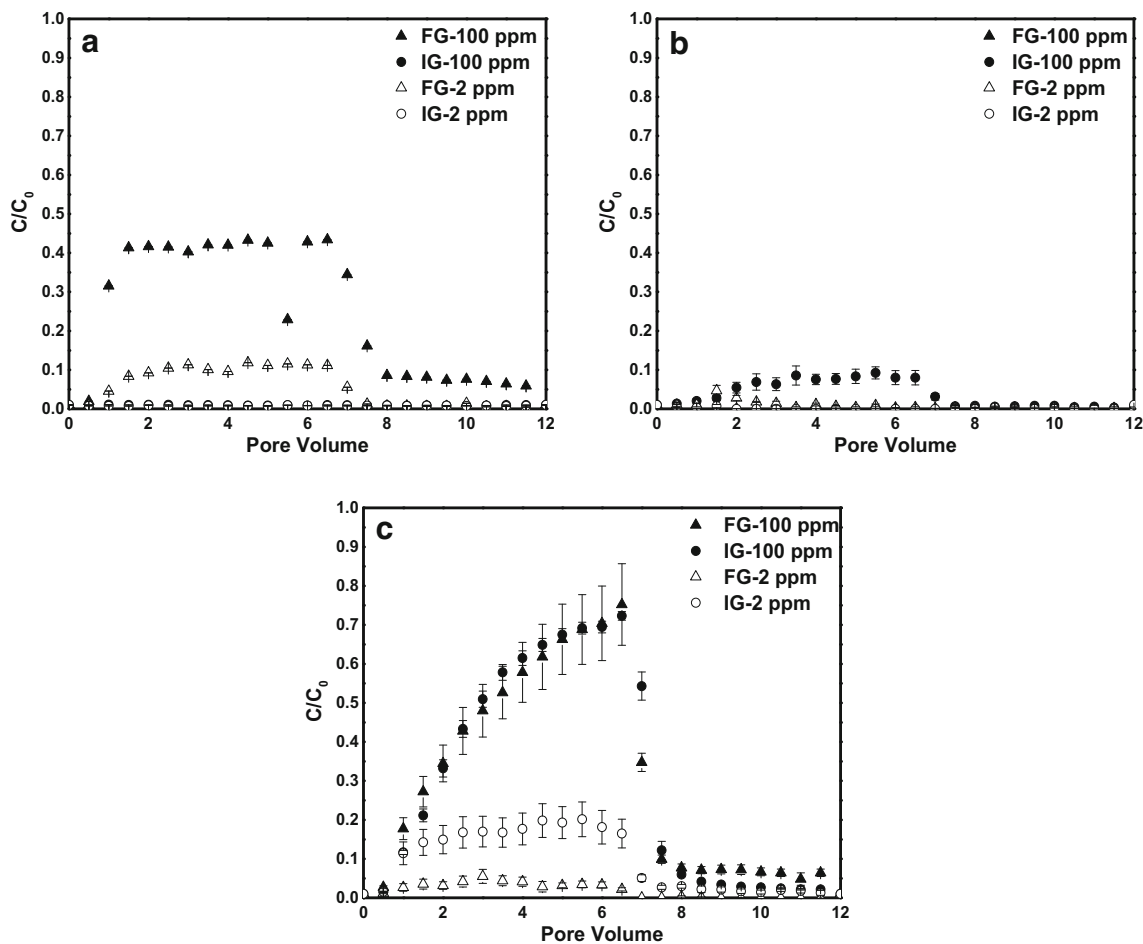


**Fig. 3** Breakthrough curves for food grade (FG) and industrial grade (IG)  $\text{TiO}_2$  nanoparticles introduced to **a** 4 mM KCl at pH 7.6, **b** 10 mM KCl at pH 6, and **c** septic effluent.  $C_0$  and  $C$  represent the influent and effluent

concentrations of  $\text{TiO}_2$ , respectively. Error bars represent standard error of triplicate measurements

distance. Unfavorable conditions ( $>435$  kT) for deposition were observed for both FG and IG  $\text{TiO}_2$  nanoparticles in 4 mM KCl apart from IG 100 ppm, where the deep primary minimum demonstrates those very favorable conditions

developed (Fig. 4a,  $-5292$  kT). For the 10 mM KCl suspensions,  $\text{TiO}_2$  nanoparticle type was significant with FG  $\text{TiO}_2$  remaining in unfavorable deposition conditions, although reduced from observations in 4 mM, while IG 2 ppm became

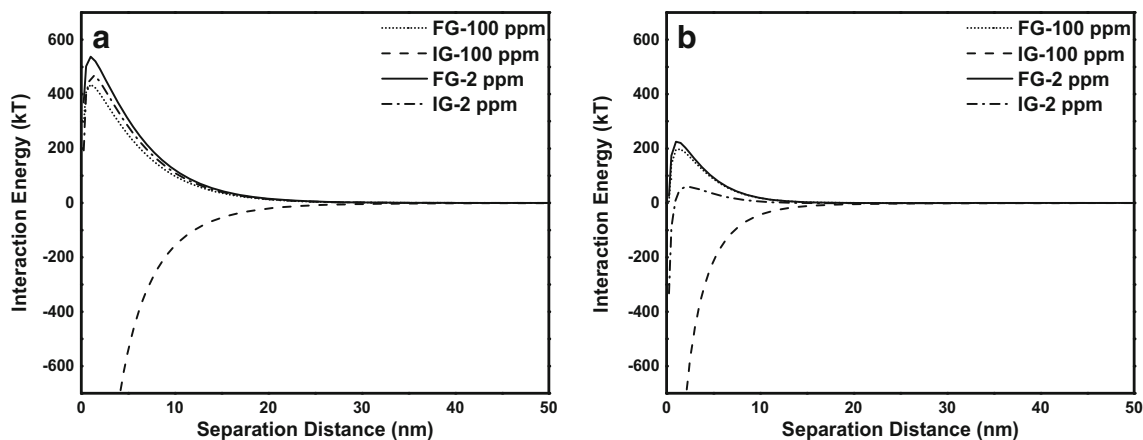


**Fig. 4** Total interaction energy profiles generated by the Derwin-Landau-Verwey-Overbeek (DLVO) theory for food grade (FG) and industrial grade (IG)  $\text{TiO}_2$  nanoparticles and the quartz sand collector surface in

both **a** 4 mM KCl at pH 7.6 and **b** 10 mM KCl at pH 6, as a function of separation distance

much closer to favorable deposition (Fig. 4b). Additionally, nanoparticle concentration affected total interaction energy with IG TiO<sub>2</sub> more than FG TiO<sub>2</sub>. FG TiO<sub>2</sub> remained unfavorable in 4 mM KCl at both particle concentrations and possessed similar interaction energy (FG 2 ppm, 225 kT; FG 100 ppm, 195 kT). Conversely, nanoparticle concentration was the difference between favorable and unfavorable deposition conditions for IG TiO<sub>2</sub> in 4 and 10 mM KCl, with unfavorable conditions for IG 2 ppm, while IG 100 ppm was favorable. Results of interaction profiles suggest that more favorable conditions for FG and IG TiO<sub>2</sub> nanoparticle deposition, at both 2 and 100 ppm concentrations, would exist in 10 mM KCl than 4 mM KCl.

## Discussion

### Nanoparticle characterization

Engineered nanomaterial interactions, and environmental behavior as a result, are very much dependent on nanoparticle stability and aggregation [30, 31]. High electrophoretic mobility ( $-4.5 \pm 0.2 \times 10^{-8}$  m<sup>2</sup>/V/s) of FG TiO<sub>2</sub> nanoparticles introduced to weak, monovalent electrolyte conditions is suggestive of a very stabilized nanoparticle (Fig. 2). Similar mobility displayed by FG TiO<sub>2</sub> was also observed in concentrated colon medium comprising proteins, carbohydrates, and mono- and divalent salts, at even at high IS (~200 mM) [23]. Between 4 and 10 mM KCl, the hydrodynamic diameter of FG TiO<sub>2</sub> remains in the range of 270 to 360 nm while IG TiO<sub>2</sub> increases to well over 1000 nm in both solutions at IG 100 ppm, which also aligns with findings from previous work conducted in high-IS, multivalent electrolyte solutions [23]. FG TiO<sub>2</sub> hydrodynamic diameters in 4 and 10 mM KCl support EPM observations of a stabilized aggregate showing that FG TiO<sub>2</sub> maintains smaller aggregate sizes than IG TiO<sub>2</sub> (Fig. 1). Di- and multivalent electrolyte suspensions are well understood to compress the electrical double layer surrounding a nanoparticle [32] and while this was observed previously with IG TiO<sub>2</sub>, FG TiO<sub>2</sub> continues to respond differently in idealized and complex solutions highlighting the significance of inherent differences [23].

Suspension pH is an additional factor capable of influencing nanoparticle stability, where particles near the IEPs are destabilized and more readily aggregate [20, 21]. The IEPs of FG and IG TiO<sub>2</sub> have been reported as pH 3.5 and 6, respectively [22]. Based on IEPs and nanoparticle concentration, the largest TiO<sub>2</sub> aggregates would be expected to form in IG 100 ppm, although this was not the case (Fig. 1). Slightly larger IG 100 ppm aggregates observed in 4 mM KCl at pH 7.6 may potentially result from a positive and reduced stability compared to 10 mM, resulting in conditions that facilitate nanoparticle aggregation (Fig. 2) [29, 33].

In wastewater treatment, organic coatings are expected to develop on nanoparticle surfaces and can impart a stabilizing effect that minimizes further aggregation [29, 30, 34, 35]. Contrary to the monovalent solutions, septic effluent represented an environment that reduced the mobility of both TiO<sub>2</sub> types; however, whereas the hydrodynamic diameter of IG TiO<sub>2</sub> nanoparticles decreased, FG TiO<sub>2</sub> aggregates became slightly larger at both 2 and 100 ppm nanoparticle concentrations (Figs. 1 and 2, respectively). Reductions in EPM and hydrodynamic diameter have been attributed to steric hindrance occurring from organic matter bound to the nanoparticle surface [31, 36] which can explain the observations for IG TiO<sub>2</sub>. These findings suggest that FG TiO<sub>2</sub> would have low retention in porous media filtration increasing the possibility of reaching groundwater.

### Column transport experiments

Findings from column breakthrough curves reveal an expectedly high rate of elution of FG TiO<sub>2</sub> nanoparticles in septic system effluent at high concentrations (Fig. 3c) [12, 14, 37]. However, environmentally relevant concentrations of nanoparticles released from septic tank may not pose an immediate risk to groundwater as FG 2 ppm was well retained inside the column. IG TiO<sub>2</sub> conversely exhibited a high degree of elution at both 2 and 100 ppm concentrations compared to the monovalent electrolyte solutions. Poor retention of IG TiO<sub>2</sub> in septic effluent compared to 4 and 10 mM KCl may potentially result from steric hindrance minimizing aggregation and deposition, allowing particles to remain in suspension [29, 30, 35, 36]. Nanomaterials have the tendency to develop organic coatings in a number of environmental settings including wastewater treatment systems [13]. Steric hindrance represents a key colloidal phenomenon that occurs with particles in aquatic solutions containing natural organic matter as the organic coatings minimize further aggregation after a certain amount of surface coverage [20]. The nanoparticle aggregate becomes stabilized by the surface attached organic polymers hindering further aggregation and deposition. As such, steric hindrance caused by the nanoparticles interacting with the biomolecules contained in the septic effluent matrix may account for the increased elution compared to the simpler salt solutions. Interestingly, findings of the current study suggest that high stability of TiO<sub>2</sub> ENMs may be a major factor in the frequency of their detection in WWTPs compared to other nanomaterials [13].

### DLVO experiments

DLVO theory was used to provide insight on the influence of van der Waals and electrostatic repulsive forces on TiO<sub>2</sub> nanoparticle interactions with quartz sand collectors during porous media transport (Fig. 4) [21, 38]. Total interaction energy

profiles determine whether favorable conditions exist for TiO<sub>2</sub> nanomaterials to deposit onto collector grains. Septic effluent exceeds the idealized solution assumption used for DLVO theory [27], so 4 mM KCl (pH 7.6) was used instead to consider effects of IS and nanoparticle concentration on interaction energy between FG TiO<sub>2</sub> and the quartz collector as a function of distance.

FG TiO<sub>2</sub> has unfavorable conditions for deposition at 2 and 100 ppm in both solutions with higher interaction energy in 4 mM KCl (max 537 kT, FG 2 ppm) (Fig. 4). Considering FG TiO<sub>2</sub> has an IEP of 3.5, exposure to pH 7.6 would result in both negatively charged nanoparticles and the collector surface ultimately inhibiting deposition [20, 27]. Similarly, FG 2 ppm TiO<sub>2</sub> also possesses the highest interaction energy (max 225 kT) although reduced from 4 mM KCl. Although FG 2 ppm developed the most unfavorable conditions for deposition in both solutions based on DLVO theory, it was observed to be the most retained nanoparticle filtration column when suspended in the septic effluent (Fig. 4). Additionally, IG 100 ppm would be expected to have highly favorable deposition in 10 and 4 mM KCl as shown in Fig. 4, yet high elution was recorded in septic effluent (Fig. 3). This suggests that organic material in water sources can potentially impart environmentally specific characteristics [30, 35] that may take precedent over inherent nanoparticle characteristics in governing nanoparticle behavior.

Engineered nanomaterials are an expanding class of emerging contaminants to environmental systems including water bodies and water treatment facilities. TiO<sub>2</sub> nanoparticles commonly incorporated into food and consumer products and subsequently released during usage have been detected at wastewater treatment facilities. As such, the impact of TiO<sub>2</sub> nanomaterials in wastewater treatment facilities was assessed using the environmentally relevant form of TiO<sub>2</sub> (food grade) and concentration (< 2 ppm) to elucidate filtration behavior of food grade TiO<sub>2</sub> nanoparticles after exiting the septic treatment system. Notably, septic effluent resulted in increased elution of both industrial and food grade TiO<sub>2</sub> at higher nanoparticle concentrations. FG TiO<sub>2</sub> was well retained at 2 ppm concentration in septic effluent, indicating that particles that escape the septic system may still be removed from the waste stream before reaching groundwater. However, particles that are eluted from the drainage field into the groundwater system are likely to be very stabilized in suspension likely resulting in greater transport. Findings of the current study provide essential insight into the significance of the solution conditions that nanoparticles are introduced to in that the potential exists for the environment to mediate differences observed between uniquely engineered nanomaterials. Future research into filtration of FG TiO<sub>2</sub> will elucidate governing mechanisms that facilitate and suppress differing behaviors between nanomaterials to better understand mechanisms governing transport of nanoparticles in porous media.

**Acknowledgements** Thanks to P. Westerhoff (ASU) for providing the nanomaterials to conduct these experiments. Any opinions, findings, and conclusions or recommendations expressed in this material are those of the author(s) and do not necessarily reflect the views of the NSF or the EPA. This work has not been subjected to EPA review, and no official endorsement should be inferred.

**Funding information** Funding from the National Science Foundation (NSF), Environmental Protection Agency (EPA), and Department of Education supported this study. T. Waller was supported by both the Department of Education (GAANN, Grant No. P200A130127) and the NSF IGERT: Water Social, Engineering, and Natural Sciences Engagement (WaterSENSE) Program (Grant No. 1144635). S. Walker's participation and work was also funded through the University of California Center for Environmental Implications of Nanotechnology (UC-CEIN), which is supported by the NSF and the EPA under Cooperative Agreement Number DBI 0830117.

## Compliance with ethical standards

**Conflict of interest** The authors declare that they have no conflicts of interests.

## References

1. Bishoge OK, Zhang L, Suntu SL, Jin H, Zewde AA, Qi Z. Remediation of water and wastewater by using engineered nanomaterials: a review. *J Environ Sci Health A*. 2018;53(6):537–54.
2. Abbas KA, Saleh AM, Mohamed A, MohdAzhan N. The recent advances in the nanotechnology and its applications in food processing: a review. *J Food Agric Environ*. 2009;7(3–4):14–7.
3. Bouwmeester H, Dekkers S, Noordam MY, Hagens WI, Bulder AS, de Heer C, et al. Review of health safety aspects of nanotechnologies in food production. *Regul Toxicol Pharmacol*. 2009;53(1):52–62.
4. Weir A, Westerhoff P, Fabricius L, Hristovski K, von Goetz N. Titanium dioxide nanoparticles in food and personal care products. *Environ Sci Technol*. 2012;46(4):2242–50.
5. Keller AA, McFerran S, Lazareva A, Suh S. Global life cycle releases of engineered nanomaterials. *J Nanopart Res*. 2013;15:1692.
6. Benn TM, Westerhoff P. Nanoparticle silver released into water from commercially available sock fabrics. *Environ Sci Technol*. 2008;42(11):4133–9.
7. Gottschalk F, Sonderer T, Scholz RW, Nowack B. Modeled environmental concentrations of engineered nanomaterials (TiO<sub>2</sub>, ZnO, Ag, CNT, fullerenes) for different regions. *Environ Sci Technol*. 2009;43(24):9216–22.
8. Brar SK, Verma M, Tyagi RD, Surampalli RY. Engineered nanoparticles in wastewater and wastewater sludge—evidence and impacts. *Waste Manag*. 2010;30(3):504–20.
9. Addo Ntim S, Norris S, Scott K, Thomas TA, Noonan GO. Consumer use effects on nanoparticle release from commercially available ceramic cookware. *Food Control*. 2018;87:31–9.
10. Crittenden JC, Trussell RR, Hand DW, Howe KJ, Tchobanoglous G. *MWH's water treatment: principles and design*. Hoboken: Wiley; 2012.
11. Bitton G. *Wastewater microbiology*. 3rd ed. Hoboken: Wiley; 2005.
12. Westerhoff P, Song GX, Hristovski K, Kiser MA. Occurrence and removal of titanium at full scale wastewater treatment plants: implications for TiO<sub>2</sub> nanomaterials. *J Environ Monit*. 2011;13(5):1195–203.
13. Westerhoff PK, Kiser A, Hristovski K. Nanomaterial removal and transformation during biological wastewater treatment. *Environ Eng Sci*. 2013;30(3):109–17.

14. Kiser MA, Westerhoff P, Benn T, Wang Y, Perez-Rivera J, Hristovski K. Titanium nanomaterial removal and release from wastewater treatment plants. *Environ Sci Technol*. 2009;43(17):6757–63.
15. Shi XM, Li ZX, Chen W, Qiang LW, Xia JC, Chen M, et al. Fate of TiO<sub>2</sub> nanoparticles entering sewage treatment plants and bioaccumulation in fish in the receiving streams. *Nano*. 2016;3-4:96–103.
16. Canter LK, Knox RC. *Septic tank system effects on ground water quality*. Chelsea: Lewis Publishers, Inc; 1985.
17. EPA US. Decentralized systems technology fact sheet: septic tank—soil adsorption systems. EPA 932-F-99-075, U S EPA. 1999.
18. Taylor AA, Walker SL. Effects of copper particles on a model septic system's function and microbial community. *Water Res*. 2015;91:350–60.
19. Waller T, Marcus IM, Walker SL. Influence of food and industrial grade TiO<sub>2</sub> nanoparticles on microbial diversity and phenotypic response in model septic system. *Environ Eng Sci*. 2018; (accepted).
20. Gregory J. *Particles in water: properties and processes*. CRC Press, Boca Raton, Florida. 2006.
21. Chowdhury I, Hong Y, Honda RJ, Walker SL. Mechanisms of TiO<sub>2</sub> nanoparticle transport in porous media: role of solution chemistry, nanoparticle concentration, and flowrate. *J Colloid Interface Sci*. 2011;360(2):548–55.
22. Yang Y, Doudrick K, Bi X, Hristovski K, Herckes P, Westerhoff P, et al. Characterization of food-grade titanium dioxide: the presence of nanosized particles. *Environ Sci Technol*. 2014;48(11):6391–400.
23. Waller T, Chen C, Walker SL. Food and industrial grade titanium dioxide impacts gut microbiota. *Environ Eng Sci*. 2017;34(8):537–50.
24. Chowdhury I, Hong Y, Walker SL. Container to characterization: impacts of metal oxide handling, preparation, and solution chemistry on particle stability. *Colloids Surf A*. 2010;368(1–3):91–5.
25. Qiu G, Au M-J, Ting Y-P. Impacts of nano-TiO<sub>2</sub> on system performance and bacterial community and their removal during biological treatment of wastewater. *Water Air Soil Pollut*. 2016;227(10):386.
26. Marcus IM, Wilder HA, Quazi SJ, Walker SL. Linking microbial community structure to function in representative simulated systems. *Appl Environ Microbiol*. 2013;79(8):2552–9.
27. Elimelech M, Gregory G, Xia X, Williams R. *Particle deposition and aggregation*, paperback ed. Oxford: Butterworth-Heinemann; 1995.
28. Fattison J, Domingos RF, Wilkinson KJ, Tufenkji N. Deposition of TiO<sub>2</sub> nanoparticles onto silica measured using a quartz crystal microbalance with dissipation monitoring. *Langmuir*. 2009;25(11):6062–9.
29. Zhang Y, Chen YS, Westerhoff P, Hristovski K, Crittenden JC. Stability of commercial metal oxide nanoparticles in water. *Water Res*. 2008;42(8–9):2204–12.
30. Chen KL, Elimelech M. Influence of humic acid on the aggregation kinetics of fullerene (C<sub>60</sub>) nanoparticles in monovalent and divalent electrolyte solutions. *J Colloid Interface Sci*. 2007;309(1):126–34.
31. Chen KL, Mylon SE, Elimelech M. Enhanced aggregation of alginate-coated iron oxide (hematite) nanoparticles in the presence of calcium, strontium, and barium cations. *Langmuir*. 2007;23(11):5920–8.
32. French RA, Jacobson AR, Kim B, Isley SL, Penn RL, Baveye PC. Influence of ionic strength, pH, and cation valence on aggregation kinetics of titanium dioxide nanoparticles. *Environ Sci Technol*. 2009;43(5):1354–9.
33. Keller AA, Wang H, Zhou D, Lenihan HS, Cherr G, Cardinale BJ, et al. Stability and aggregation of metal oxide nanoparticles in natural aqueous matrices. *Environ Sci Technol*. 2010;44(6):1962–7.
34. Chowdhury I, Duch MC, Mansukhani ND, Hersam MC, Bouchard D. Colloidal properties and stability of graphene oxide nanomaterials in the aquatic environment. *Environ Sci Technol*. 2013;47(12):6288–96.
35. Chowdhury I, Walker SL, Mylon SE. Aggregate morphology of nano-TiO<sub>2</sub>: role of primary particle size, solution chemistry, and organic matter. *Environ. Sci.: Processes Impacts*. 2013;15(1):275–82.
36. Chowdhury I, Cwiertny DM, Walker SL. Combined factors influencing the aggregation and deposition of nano-TiO<sub>2</sub> in the presence of humic acid and bacteria. *Environ Sci Technol*. 2012;46(13):6968–76.
37. Giese B, Klaessig F, Park B, Kaegi R, Steinfeldt M, Wigger H, et al. Risks, release and concentrations of engineered nanomaterial in the environment. *Sci Rep*. 1565;8(1):2018.
38. Bradford SA, Kim HN, Haznedaroglu BZ, Torkzaban S, Walker SL. Coupled factors influencing concentration-dependent colloid transport and retention in saturated porous media. *Environ Sci Technol*. 2009;43(18):6996–7002.



**Travis Waller** has just completed his Ph.D. in Chemical and Environmental Engineering from the University of California, Riverside. His research area focuses on nanoparticle interactions in microbially driven environments such as that found in biological water treatment systems. He is additionally interested in developing student-centered strategies for engineering education that ease the learning process.



**Ian M. Marcus** is a project scientist in the Bourns College of Engineering at the University of California, Riverside. His research focuses on changes to dynamic biological systems post-external perturbations, and developing student-centric curriculum in engineering.



**Sharon L. Walker** is the John Babbage Chair in Environmental Engineering and Professor of Chemical and Environmental Engineering at the University of California, Riverside, and Fellow of the Association for Environmental Engineering and Science Professors. Her work applies fundamental colloid science, chemical, and environmental engineering concepts to challenges in water treatment as it applies to water treatment, reuse, and food safety.